GSA Data Repository Item 2019243

Baker, S.J., Belcher, C.M., Barclay, R.S., Hesselbo, S.P., Laurin, J., and Sageman, B.B., 2019, CO_2-induced climate forcing on the fire record during the initiation of Cretaceous oceanic anoxic event 2: GSA Bulletin, https://doi.org/10.1130/B35097.1.

Data Repository

Table DR1. Age control points used in this study.

Table DR2. Charcoal abundances from this study; study collection site, local stratigraphic height (as used in Barclay et al., 2010), calculated age, sample lithology and stomatal index results from Barclay et al. (2010) with estimated ages.

Figure DR1. Image of charcoal taken under a binocular light microscope, illustrating key identification characteristics of charcoal compared with the brownish hues of vegetal matter.

Figure DR2. Charcoal data from this study analysed from within the Dakota Fm, plotted against $\delta^{13}C$ organic curve and estimated changes in CO_2 after Barclay et al. (2010) across the initiation of OAE2, displayed as total charcoal counts per 10g bulk rock, and total charcoal counted per 1g of total organic matter remaining after demineralization. Note the change in scale between the counted charcoal and the calculated abundance per g/TOM.

Figure DR3. (A) Cross-plot of total >125μm charcoal abundance counted per 10g against total organic matter in 10g sample, illustrating no correlation between char abundances and total organic matter, nor within different facies. (B) Cross-plot of total >125μm charcoal abundance counted per 10g against total organic matter in 10g sample at the different sample locations, illustrating no correlation between char abundances and total organic matter found at different localities.

Table DR 1. Age control points used in this study. [1]) Meyers et al. (2012b); USGS #1 Portland core; [2]) Sageman et al. (2006); USGS #1 Portland core; [3]) Ma et al. (2014); Aristocrat Angus core; [4]) applies to the Kaiparowits Plateau only; detailed correlation to Big Hill uncertain; [5]) Barclay et al. (2015); Henrieville section; [6]) Laurin et al. (in review); Big Hill section.

Age control point	Stratigraphic level at Big Hill (m)	Numerical Age (Myr)	Uncertainty (Myr)	Floating age relative to base Turonian (Myr)	Floating age relative to bentonite A (Myr)	Age model (Myr)
Base TURONIAN	77	93.90 [1])	+0.07/-0.09	0		93.90
Bentonite B	73	94.07 [1])	+0.16/-0.15			94.07
Marlstone LS5/LS6	69			0.23 [2])		94.13
Base N. juddii Zone	56.5			0.30 [2])		94.20
Bentonite A	39	94.27 [1])	+0.16/-0.17	0.37 [2])	0	94.27
Bentonite sub-PBC-3	31			0.42 [2])		94.32
Base positive CIE (onset OAE2)	6.5				0.17 [3])	94.44
Base negative CIE (precursor)	1.6				0.21 [3])	94.48
Bentonite KJ08142	-- [4])	94.88 [5])	±0.11			94.88
Bentonite KJ08143	-- [4])	95.07 [5])	±0.12			95.07
Bentonite BH2015	-118	95.98 [6])	±0.12			95.98

Table DR 2. Charcoal abundances from this study; study collection site, local stratigraphic height (as used in Barclay et al., 2010), calculated age, sample lithology and stomatal index results from Barclay et al. (2010) with estimated ages.

Sample ID	**Collection Site**	**Local Stratigraphic height (as in Barclay et al., 2010)**	**Sample lithology for samples analysed for charcoal abundances**	**Model age (Myr ago)**	**Charcoal count per 1g of total organic matter**	***Hypodaphnis zenkeri*** **CO_2 = (–27.447 × SI_{fossil}) + 559.67** **(Barclay et al., 2010)**	***H.zenkeri*** **–95%CI** **(Barclay et al., 2010)**	**H.zenkeri +95%CI** **(Barclay et al., 2010)**	***Laurus nobilis*** **(Transformed) Predicted CO_2** **CO_2 = [–168.39 × Ln(SI_{fossil})] + 790.93** **(Barclay et al., 2010)**	***L. nobilis*** **–95%CI** **CO_2 = (-9.3347 × SI_{fossil}) + 467.28** **(Barclay et al., 2010)**	**L. nobilis +95%CI** **CO_2 = (-9.3347 × SI_{fossil}) + 467.28** **(Barclay et al., 2010)**
RSB0763	Moreno Hill, New Mexico	74.9		~93.0 (approximate age; top of M. nodosoides zone; Barclay 2011)	-	318	303	330	424	385	472
RSB0552_CDR2 58.8B	Big Hill 'Upper'	58.5	Organic rich mudstone	94.100	35	-	-	-	-	-	-
RSB0552_CDR2 36.0A	Big Hill 'Upper'	36.0	Organic rich mudstone	94.230	15	-	-	-	-	-	-
MPC14	Maple Canyon	29.9		~94.22 (uncertainty +-20kyr relative to Big Hill samples)	-	405	362	574	473	405	536
RSB0527_CDR4 24.76A	Big Hill 'Lower'	24.76	Siltstone	94.346	8	-	-	-	-	-	-
MPC32	Maple Canyon	20.4		~94.26 (uncertainty +-20kyr relative to Big Hill samples)		397	361	519	468	404	529
CDR4_17.62A	Big Hill 'Lower'	17.62		94.382	-	318	307	334	425	385	475
RSB0527_CDR4 16.9A	Big Hill 'Lower'	16.9	Claystone	94.385	186	-	-	-	-	-	-

Sample ID	**Collection Site**	**Local Stratigraphic height (as in Barclay et al., 2010)**	**Sample lithology for samples analysed for charcoal abundances**	**Model age (Myr ago)**	**Charcoal count per 1g of total organic matter**	***Hypodaphnis zenkeri*** **CO_2 = (–27.447 × SI_{fossil}) + 559.67** **(Barclay et al., 2010)**	***H.zenkeri* –95%CI** **(Barclay et al., 2010)**	**H.zenkeri +95%CI** **(Barclay et al., 2010)**	***Laurus nobilis* (Transformed) Predicted CO_2** **CO_2 = [–168.39 × Ln(SI_{fossil})] + 790.93** **(Barclay et al., 2010)**	***L. nobilis* –95%CI** **CO_2 = (-9.3347 × SI_{fossil}) + 467.28** **(Barclay et al., 2010)**	**L. nobilis +95%CI** **CO_2 = (-9.3347 × SI_{fossil}) + 467.28** **(Barclay et al., 2010)**
RSB0527_CDR4 10.6A	Big Hill ‘Lower’	10.6	Organic rich mudstone	94.417	6947	-	-	-	-	-	-
RSB0527_CDR4 10.0A	Big Hill ‘Lower’	10.0	Organic rich mudstone	94.420	1446	440	357	688	497	414	563
RSB0527_CDR4 6.8A	Big Hill ‘Lower’	6.8	Organic rich mudstone	94.436	5965	389	359	500	464	402	525
CDR4-5.2A	Big Hill ‘Lower’	5.2		94.449	-	461	345	795	515	419	582
RSB0527_CDR4 2.4A	Big Hill ‘Lower’	2.4	Organic rich mudstone	94.474	24	485	329	903	533	424	599
RSB0749_10.35M	Kanarra Mountains	-0.55	Organic rich mudstone	94.466	750	-	-	-	-	-	-
RSB0749_8.63M	Kanarra Mountains	-1.17	Organic Claystone	94.482	916	-	-	-	-	-	-
RSB0543_CWC1_MINUS 2.7A	Cottonwood Canyon	-1.2	Organic claystone	94.575	233	417	362	601	482	409	547
RSB0749-8.43	Kanarra Mountains	-1.4		94.484	-	354	340	397	443	393	498
RSB0749_8.23M	Kanarra Mountains	-1.6	Organic claystone	94.487	129	-	-	-	-	-	-
RSB0749_7.63M	Kanarra Mountains	-2.2	Organic claystone	94.495	143	413	362	574	478	407	541
RSB0543_CWC1_MINUS 1.2A	Cottonwood Canyon	-2.7	Organic claystone	94.535	267	306	290	317	419	382	466
RSB0749_5.73M	Kanarra Mountains	-3.9	Claystone	94.519	9	-	-	-	-	-	-
RSB0749_5.6M	Kanarra Mountains	-4.1	Organic claystone	94.520	29	-	-	-	-	-	-
RSB0749_1.43M	Kanarra Mountains	-8.3	Organic claystone	94.572	10	-	-	-	-	-	-

Sample ID	**Collection Site**	**Local Stratigraphic height (as in Barclay et al., 2010)**	**Sample lithology for samples analysed for charcoal abundances**	**Model age (Myr ago)**	**Charcoal count per 1g of total organic matter**	***Hypodaphnis zenkeri*** **CO_2 = (–27.447 × SI_{fossil}) + 559.67** **(Barclay et al., 2010)**	***H.zenkeri*** **–95%CI** **(Barclay et al., 2010)**	**H.zenkeri +95%CI** **(Barclay et al., 2010)**	***Laurus nobilis*** **(Transformed) Predicted CO_2** **CO_2 = [–168.39 × Ln(SI_{fossil})] + 790.93** **(Barclay et al., 2010)**	***L. nobilis*** **–95%CI** **CO_2 = (-9.3347 × SI_{fossil}) + 467.28** **(Barclay et al., 2010)**	**L. nobilis +95%CI** **CO_2 = (-9.3347 × SI_{fossil}) + 467.28** **(Barclay et al., 2010)**
RSB0749_1.18M	Kanarra Mountains	-8.7	Organic claystone	94.576	555	-	-	-	-	-	-
CWC2-m18.5-spec.1	Cottonwood Canyon	-18.5		94.788	-	413	362	574	477	407	541
RSB0738	Wahweap Creek	-18.8	Organic rich mudstone	94.721	10	-	-	-	-	-	-
RSB0735	Wahweap Creek	-23.8	Organic rich mudstone	94.900	0	-	-	-	-	-	-
RSB0733	Wahweap Creek	-26.9	Organic rich mudstone	94.955	36	-	-	-	-	-	-
CWC-m27.7A	Cottonwood Canyon	-27.7		95.000	-	370	351	438	452	397	510
RSB0731	Wahweap Creek	-31.6	Organic rich mudstone	95.042	86	-	-	-	-	-	-
RSB0730	Wahweap Creek	-31.7		95.042	-	338	327	365	435	390	487
RSB0727	Wahweap Creek	-39.9	Mudstone	95.194	21	334	321	355	432	389	483
RSB0534-9.0A	Bald Knoll Mine	-61.0		~95.2 (position relative to the oldest sample from Wahweap Creek uncertain)	-	314	300	327	423	384	471

Figure DR 1 Image of charcoal taken under a binocular light microscope, illustrating key identification characteristics of charcoal compared with the brownish hues of vegetal matter.

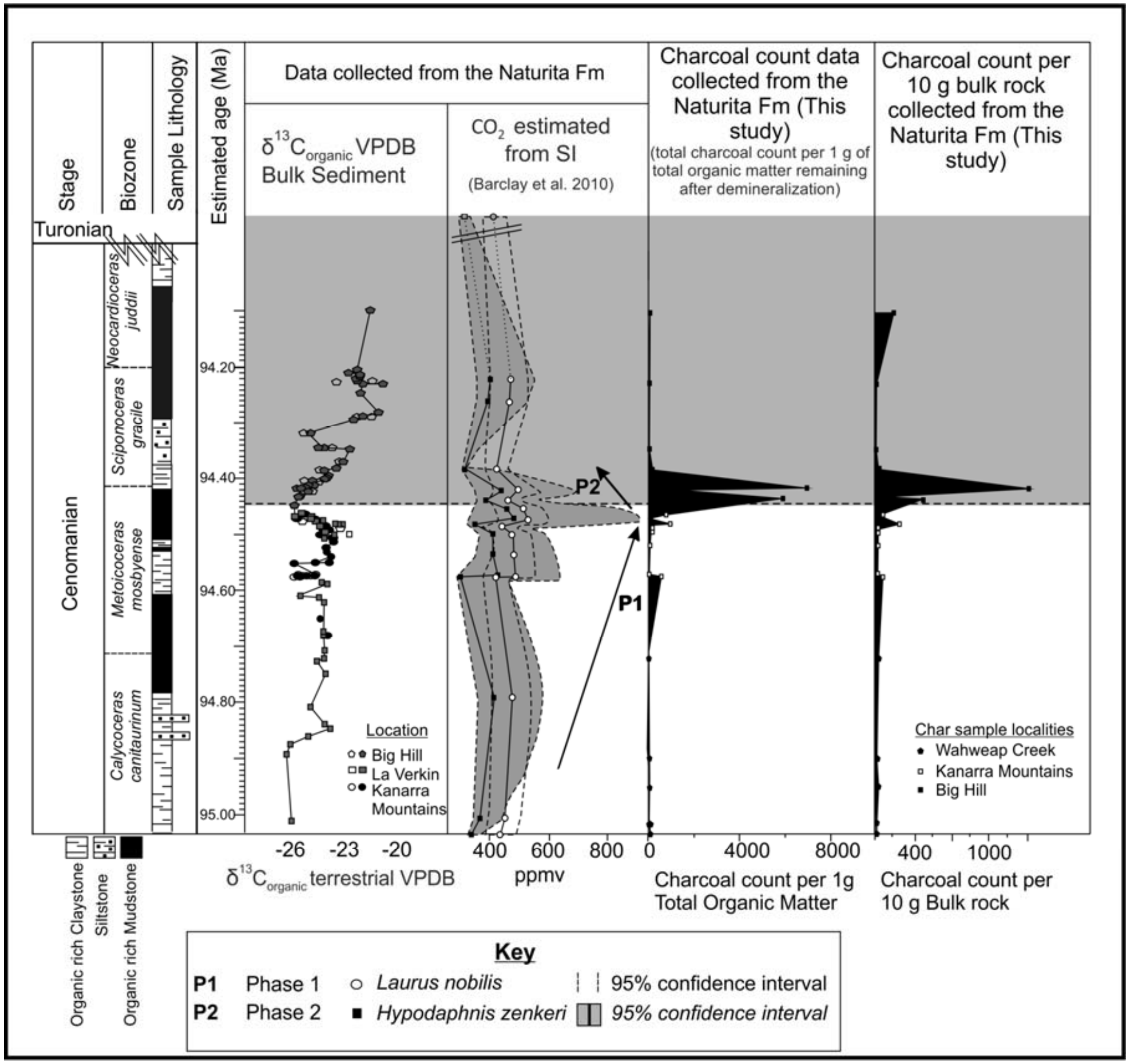

Figure DR 2 Charcoal data from this study analysed from within the Dakota Fm, plotted against $\delta^{13}C$ organic curve and estimated changes in CO_2 after Barclay et al. (2010) across the initiation of OAE2, displayed as total charcoal counts per 10g bulk rock, and total charcoal counted per 1g of total organic matter remaining after demineralization. Note the change in scale between the counted charcoal and the calculated abundance per g/TOM.

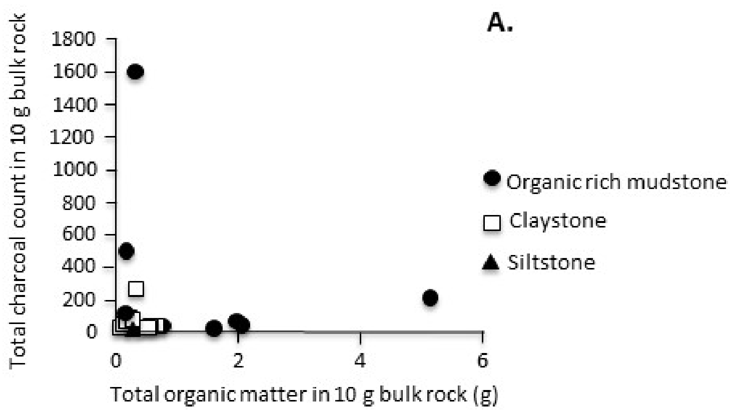

Figure DR 3 A. Cross-plot of total >125µm charcoal abundance counted per 10g against total organic matter in 10g sample, illustrating no correlation between char abundances and total organic matter, nor within different facies.

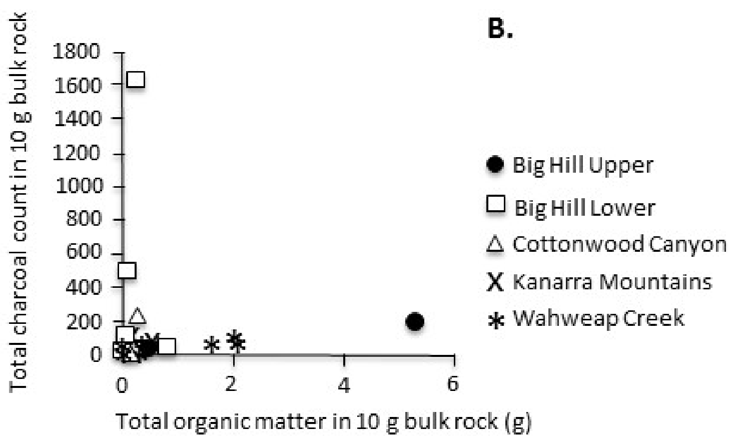

Figure DR 3 B. Cross-plot of total >125µm charcoal abundance counted per 10g against total organic matter in 10g sample at the different sample locations, illustrating no correlation between char abundances and total organic matter found at different localities.